Neotropical Ichthyology

Original article

https://doi.org/10.1590/1982-0224-2022-0102

Early life history of two Neotropical Triportheidae fish (Characiformes)

Ruineris Almada Cajado[1,2], Fabíola Katrine Souza Silva[1,3], Lucas Silva Oliveira[1,4], Zaqueu dos Santos[1,3], Andréa Bialetzki[5] and Diego Maia Zacardi[1,3]

Correspondence:
Ruineris Almada Cajado
ruineris.cajado@gmail.com

The early ontogeny of *Triportheus albus* and *T. angulatus*, two fish species of Triportheidae, is described using morphological, meristic, and morphometric characters. These species are exploited by subsistence fisheries and have potential as an alternative source of fish, given the decline in the natural stocks of other commercially important fish species in the Amazon. The specimens were collected in the open water limnetic zone, under of the macrophyte stands, and in subsurface areas near sandbars in the Amazon basin. Intra and interspecific morphometric analyzes were performed to evaluate growth models between species. The combination of color pattern, body morphology, morphometric proportions and myomeres number distinguishes the species from each other and from other congeners. Some morphometric relationships related to head as snout length and eye diameter as well as length from the snout to the origins of anal and length from the snout to the origins of pelvic, related with standard length were different between the two species of *Triportheus*, reflecting different growth models between them. An identification key for larvae and juveniles of some species of *Triportheus* from the Eastern Amazon is presented.

Keywords: Fish larvae, Identification key, Morphology, *Triportheus albus*, *Triportheus angulatus*.

Submitted October 24, 2022
Accepted March 7, 2023
by Fernando Carvalho
Epub April 14, 2023

1 Laboratório de Ecologia do Ictioplâncton e Pesca em Águas Interiores, Instituto de Ciências e Tecnologia das Águas, Universidade Federal do Oeste do Pará, Rua Vera Paz, Salé, 68040-255 Santarém, PA, Brazil. (RAC) ruineris.cajado@gmail.com (corresponding author), (FKSS) fabiola.katrine@gmail.com, (LSO) lucasmdcpa@gmail.com, (ZS) zaqueu_sant@hotmail.com, (DMZ) dmzacardi@hotmail.com.

2 Programa de Pós-Graduação em Ecologia Aquática e Pesca, Núcleo de Ecologia Aquática e Pesca da Amazônia, Universidade Federal do Pará, Av. Perimetral, 2651, 66040-830 Belém, PA, Brazil.

3 Programa de Pós-Graduação em Biodiversidade, Instituto de Ciências e Tecnologia das Águas, Universidade Federal do Oeste do Pará, Rua Vera Paz, Salé, 68040-255 Santarém, PA, Brazil.

4 Programa de Pós-Graduação em Ecologia, Instituto de Ciências Biológicas-ICB, Universidade Federal do Pará, Av. Perimetral, 2651, 66040-830 Belém, PA, Brazil.

5 Laboratório de Ictioplâncton-Núcleo de Pesquisas em Limnologia, Ictiologia e Aquicultura (Nupélia), Centro de Ciências Biológicas, Universidade Estadual de Maringá, Avenida Colombo, 5790, 87020-900 Maringá, PR, Brazil. (AB) bialetzki@nupelia.uem.br.

Online version ISSN 1982-0224
Print version ISSN 1679-6225

Neotrop. Ichthyol.
vol. 21, no. 1, Maringá 2023

A ontogenia inicial de *Triportheus albus* e *T. angulatus*, duas espécies de peixes pertencentes a Triportheidae, é descrita usando caracteres morfológicos, merísticos e morfométricos. Essas espécies são exploradas pela pesca de subsistência e têm potencial como fonte alternativa de pescado, dado o declínio nos estoques naturais de outras espécies de peixes comercialmente importantes na Amazônia. Os espécimes foram coletados na zona limnética de águas abertas, sob bancos de macrófitas e em áreas subsuperficiais próximas a bancos de areia na bacia amazônica. Análises morfométricas, intra e interespecíficas, foram realizadas para avaliar modelos de crescimento entre as espécies. A combinação do padrão de coloração, morfologia corporal, proporções morfométricas e número de miômeros distingue as espécies entre si e de outras congêneres. Algumas relações morfométricas relacionadas à cabeça, como comprimento do focinho e diâmetro do olho, assim como o comprimento do focinho à origem da nadadeira anal e o comprimento do focinho à origem da nadadeira pélvica, relacionadas ao comprimento padrão foram diferentes entre as duas espécies de *Triportheus*, refletindo modelos distintos de crescimento entre elas. Uma chave de identificação para larvas e juvenis de algumas espécies de *Triportheus* da Amazônia Oriental é apresentada.

Palavras-chave: Chave para identificação, Larva de peixe, Morfologia, *Triportheus albus*, *Triportheus angulatus*.

INTRODUCTION

The *Triportheus* Cope, 1872, popularly known as narrow hatchet fish and elongate hatchet fish, comprises small teleost fish exclusive to the Neotropical region (Malabarba, 2004). Species of this genus can be easily distinguished by the presence of long pectoral fins, expanded coracoid bones, and lateral line with a pronounced postventral slope close to the pectoral fin (Van der Sleen, Zanata, 2018). They are pelagic fish, perform medium-distance migrations for reproductive purposes, usually between September and October, and have omnivorous feeding habits (Doria, Queiroz, 2008; García-Dávila *et al*., 2018; Silvano *et al*., 2020).

In the Amazon River and its tributaries are recorded eight species of this genus– *Triportheus albus* Cope, 1872, *T. angulatus* (Spix & Agassiz, 1829), *T. auritus* (Valenciennes, 1850), *T. brachipomus* (Valenciennes, 1850), *T. culter* (Cope, 1872), *T. curtus* (Garman, 1890), *T. pictus* (Garman, 1890), and *T. rotundatus* (Jardine, 1841) (Dagosta, Pinna, 2019). Among these species, *T. auritus*, *T. albus*, and *T. angulatus* stand out for their high abundance, being frequently recorded in several biotopes in the white, clear, and black waters of the Amazon basin (Araújo *et al*., 2017; Imbiriba *et al*., 2020; Silvano *et al*., 2020). These species are widely used as a source of protein by riverine populations in subsistence fishing along the Solimões-Amazonas system channel and its tributaries (Batista *et al*., 2012; Isaac *et al*., 2016; Zacardi, 2020). Additionally, they are becoming increasingly common in regional markets as an alternative to meet the demand for fish despite the accelerated decline of other widely exploited species (Batista *et al*., 2012; Ferraz, Barthem, 2016; Isaac *et al*., 2016).

Despite the ecological relevance and economic potential of these species, information about their phenotype during early ontogeny is incipient, with just over 22% of the 18 species of *Triportheus* having their embryonic and/or larval stages described (Reynalte-Tataje *et al*., 2020; Fricke *et al*., 2022). In the Amazon basin, only *T. auritus* had its initial development characterized (Cajado *et al*., 2021), while Oldani (1979) and Garcia *et al.* (2016) presented a succinct and incomplete description of the early life stages of *T. paranensis* (both currently = *T. nematurus*) and *T. angulatus* (*T. nematurus*/*T. signatus sensu* Lopes, 2020) in the Paraná River basin.

Integrative approaches that describe the morphological, meristic, and morphometric characters of the different ontogenetic phases are fundamental for the accurate identification of the initial stages of fish development and an important step for studies on ichthyoplankton ecology and fisheries biology (Reynalte-Tataje *et al*., 2020; Zacardi *et al*., 2020a,b). The difficulty in identifying the material collected in nature is one of the larger obstacles encountered in ichthyoplankton studies, due to the intense interspecific similarity of fish during the initial life cycle (Cajado *et al*., 2021; Lima *et al*., 2021; Silva *et al*., 2021; Oliveira *et al*., 2022).

Here, we intend to expand the basic knowledge of the early ontogeny of Neotropical fish, through the detailed description of larvae and juveniles of *T. angulatus* and *T. albus* that occur in the Amazon basin. This study was based on morphology, meristic counts and morphometric measurements, and estimated the growth patterns throughout the early development of the two species. Furthermore, we propose an identification key for these two species and other congeners that occur in sympatry approaching the early ontogeny.

MATERIAL AND METHODS

Collection of biological material. The larvae and juveniles of fish used in this study came from sampling carried out in the middle stretch of the Solimões River and lower Japurá River, around the Mamirauá Sustainable Development Reserve (Reserva de Desenvolvimento Sustentável de Mamirauá) - MSDR (03°08'S 64°45'W and 02°36'S 67°13'W) in the state of Amazonas. Also, in the lower Amazon River in the state of Pará: (1) open water limnetic zone (02°28'42"S 54°38'04"W); (2) under macrophyte stands in lakes (02°26'44"S 54°16'53"W) and (3) lake channels in floodplain areas (02°12'41"S 54°45'42"W and 02°18'52"S 54°43'11"W). In addition to collections along the lower and middle stretch of the Tapajós River, Pará, Brazil (02°28'46"S 55° 04'34"W and 05°32'47"S 57°05'35"W) and in different periods (Rise, flood, drought e fall) (Fig. 1).

The larvae and juveniles were collected for 12 years, between 2010 and 2022, by horizontal trawling in the subsurface of the water column (open water) using a conical-cylindrical plankton net (0,3 mm mesh). For sampling in macrophyte stands floating was used sieve fish net (0,5 mm mesh) of 1.0 x 1.5 x 1.0 m, while for sampling near sandbanks and marginal areas of rivers and lakes was used a seine net (1 mm mesh) of 5 m x 1.5 m.

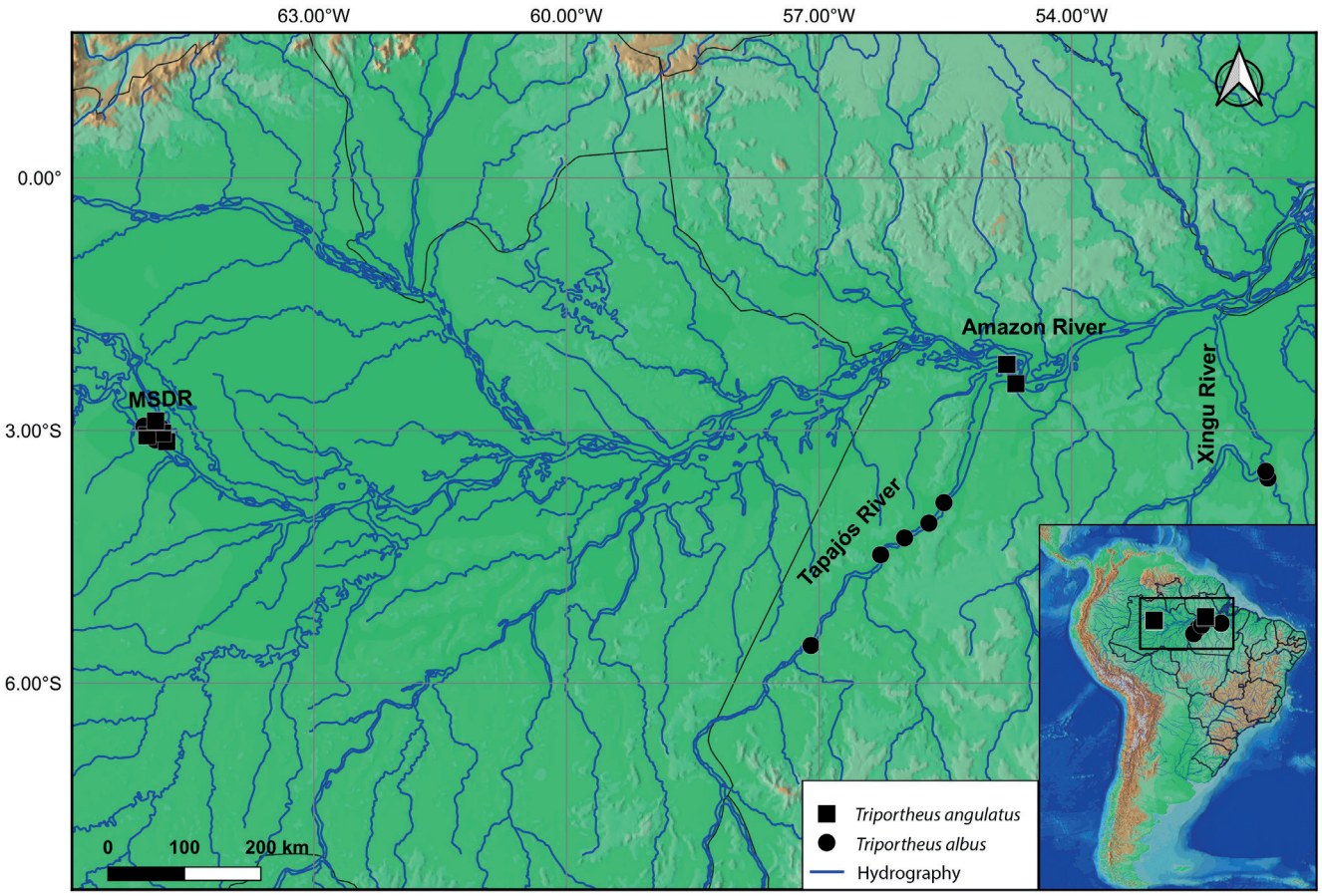

FIGURE 1 | Map of the Eastern Amazon, showing the capture sites of the *Triportheus* used in the study. MSDR: Mamirauá Sustainable Development Reserve.

Analysis of biological material. After capture, the specimens were euthanized with benzocaine (250 mg/L) and fixed in a 10% formalin solution buffered with calcium carbonate. In the laboratory, *Triportheus* larvae and juveniles were sorted, separating them from plant material and plankton, then identified at the species level, using the regressive developmental sequence technique from the known juveniles to the smallest individuals, as suggested by Nakatani *et al*. (2001). The juveniles were identified using specific literature (Malabarba, 2004). After identification, the specimens were classified according to their degree of development as proposed by Ahlstrom *et al*. (1976) and modified by Nakatani *et al*. (2001) in larval (preflexion, flexion, and postflexion stages) and juvenile periods.

The description of the larval and juvenile periods was based on the observation of the main morphological events and the degree of initial development, in addition to meristic and morphometric characters, and the individuals that best represented the characteristics of the species were photographed and illustrated. It is noteworthy that the choice of the best individuals was based on the integrity of the specimen, considering the state of the fins, body shape, and the presence or absence of pigmentation (in this case, we chose the individuals that best represented the patterns observed for the species

at a certain stage of development). Moreover, voucher specimens were deposited in the Coleção de Referência de Ovos e Larvas de Peixes, Laboratório de Ecologia do Ictioplâncton e Pesca em Águas Interiores (CROLP LEIPAI), Universidade Federal do Oeste do Pará (https://specieslink.net/col/CROLP-LEIPAI/), LEIPAI 397 to LEIPAI 431 (*T. angulatus*), and LEIPAI 432 to LEIPAI 459 (*T. albus*).

Data analysis. Morphometric measurements (expressed in mm) were performed using a binocular stereomicroscope (Leica S9i) coupled to an integrated digital color camera for image capture and analysis – software (Leica LAS EZ). Eleven morphometric characters were measured (Ahlstrom *et al*., 1976): head depth (HD), body depth (BD), head length (HL), snout length (SNL), standard length (SL), eye diameter (ED) and the length from the snout to the origins of anal (SNA), dorsal (SND), pectoral (SNP), and pelvic (SNV) fins. Additionally, the depth of the body toward the anus (BDA) was measured. Notably for SND and SNA in the preflexion stage, the distance from the snout to the beginning of the embryonic dorsal fin and the beginning of this membrane after the anus were considered, respectively. For meristic characterization, we counted the preanal, postanal and total number of myomeres, and the number of unbranched rays and/or branched rays present in anal (A), dorsal (D), pectoral (P), and pelvic (V) fins.

For the analysis of morphometric relationships of larvae and juveniles (expressed as a percentage), the variables HD, SNL, and ED were related to HL, while BD, BDA, HL, SNA, SND, SNP, and SNV were related to SL. Body relationships for BD (BD/SL), HL (HL/SL), and ED (ED/HL) were established using the criteria suggested by Leis, Trnski (1989). Additionally, the proportions of HD in relation to BDA and BD were explored to better understand the morphometric relationships throughout development.

To evaluate body growth patterns, regression models were used in which the morphometric variables (dependent), except BDA, were plotted in relation to SL and HL (independent variables). These relationships were described by different growth models, which may indicate relevant biological processes linked to early ontogeny (Kováč *et al*., 1999). The hypothesis of continuous isometric growth was tested using a simple linear regression model. Two alternative developmental hypotheses were also tested: gradual allometric growth (quadratic regression) and discontinuous isometric growth (piecewise linear regression – characterized by breakpoints that highlight divergent growth rates). The selection of the best model for each analyzed relationship was based on the F test, with a significance level of $p < 0.05$.

The statistical significance of differences between morphometric variables was assessed using an Analysis of Covariance (ANCOVA), were HD, SNL, ED, BD, HL, SND, SNA, SNV, and SNP were response variables and SL, and HL were covariates. Before performing the ANCOVA, the data were transformed into log and a significance level of $p < 0.05$ was adopted. Regression analyses were performed using StatisticaTM 7.0 software StartSoft and the ANCOVA was performed using software *R* version 4.1.1.

RESULTS

A total of 248 specimens were analyzed 104 of *Triportheus albus* (25 preflexion, 18 flexion, 45 postflexion, and 16 juveniles) and 143 of *T. angulatus* (46 preflexion, 54 flexion, 13 postflexion, and 30 juveniles). Yolk sac larvae of both species were not found during sampling. Individuals in the early stages, such as preflexion and flexion, were captured mainly in open water. In contrast, the more developed ones (*e.g.*, postflexion and juveniles) were caught under macrophyte stands and in shallow and marginal areas of rivers and lakes.

Triportheus albus

Larval period. Preflexion (Figs. 2A-B):The standard length ranges from 3.29 to 6.13 mm (mean ± SD = 4.74 mm ± 0.77). The notochord is rectilinear and visible through transparency. There are no traces of the yolk sac. The body is elongated in a fusiform shape, the dorsal profile concave, and the head less deep than the trunk (HD/BD - 72.79 to 99.26%, mean ± SD = 89.11 ± 6.70%). The snout is rounded, but at the end of the stage, it becomes pointed; the mouth is superior and the inferior jaw long, with the entire dentary exposed when in dorsal view. The nostrils are simple, and the operculum is formed. The eyes are spherical and completely pigmented. The swim bladder is inflated and takes up a great space in the abdomen. There are pigments involving the swim bladder upper portion and, rarely, the lateral region of the digestive tube. Chromatophores are observed in the ventral region, located at the anterior portion of the digestive tube, sometimes in the median region, little conspicuous under it and abundant posteriorly the anus, but without reaching the caudal peduncle. In individuals larger than 4.50 mm SL, scarce punctate pigments appear in the dorsal fin region and parallel to the notochord. The finfold is hyaline, involves the body dorsoventrally from the second half of the intestine to the midline of the stomach (SND/SL - 41.43 to 51.37%, mean ± SD = 46.72 ± 2.52). Only the pectoral fin button is present. The total myomeres number ranges from 38 to 39 (18–19 preanal and 19–21 postanal).

Flexion (Figs. 2C–D): The standard length ranges from 6.15 to 9.13 mm (mean ± SD = 7.73 mm ± 0.95). The notochord tip is flexed by the appearance of the hypural plate. The body remains in the fusiform shape, whose trunk is the highest part, but without a sharp angle between the anterior and posterior regions. Snout, mouth, maxilla, nostrils, eyes, swim bladder, and pectoral fin did not show any changes. The anus is located posteriorly to the middle of the body. The color pattern is similar to the previous stage, however, the pigmentation parallel to the notochord, in the ventral and cephalo-dorsal regions, becomes more conspicuous. This dorsal pigmentation extends in a band of sparse chromatophores, dendritic on the cephalic plate and punctate on the dorsum, to the place of origin of the adipose fin, but never over the urostyle. Few punctate pigments (rarely dendritic) are observed in the snout, premaxilla, dentary, and in more developed individuals, at the base of the caudal rays. Internal melanophores also appear along the cleithrum at the base of the pectoral fin. In this stage, there is the odd fins delineation and the formation of their rays, which at the end of the stage are, for the most part, developed. Similarly, the finfold is observed only in the region of the pelvic

fin origin. The adipose fin is in development. The caudal rays begin to segment, and the shape of the caudal fin is modified, initiating the division into two lobes. The total myomeres number ranges from 38 to 39 (18–22 preanal and 17–20 postanal).

Postflexion (Figs. 2E–F): The standard length ranges from 10.22 to 18.91 mm (mean ± SD = 13.82 mm ± 2.63). The notochord and swim bladder are no longer visible through transparent because the muscle tissue. At the beginning of the stage, the shape of the body resembles flexion, but during development, the appearance of the ventral keel is observed, and the body acquires a deep and compressed shape. The nostrils become double. Initially, the pigmentation is conspicuous, enhancing the pattern of the previous stage, but punctiform and dendritic chromatophores appear through the maxilla, operculum, pre-operculum, around the eyes, on the inner part of the lateral surface of the digestive tract, and in rays of the odd fins, except the adipose fin. In individuals larger than 14.00 mm SL, pigments are observed in the pectoral unbranched ray. At the end of the stage, bands are formed in the dorsal and mediolateral regions of the body, which extend from the snout and pre-operculum, respectively, to the caudal peduncle. Additionally, caudal fin pigmentation becomes more concentrated at the ends of the rays. The midline under region of the body is almost hyaline and when appear pigments, these are concentrated at the caudal fin base. In this stage, the appearance of the scales is observed, which have pigmented distal edge. The odd fins are in the final stage of branching and segmentation of the flexible rays and the adipose fin is already formed. There are remnants of the finfold in the ventral region. At 10.22 mm SL, the first pectoral fin rays are observed. At 12.00 mm SL the pelvic fin rays appear, but still do not have all the formed and segmented elements. The myomeres total number range from 38 to 39 (17–18 preanal and 21–22 postanal), while unbranched rays and branched range from ii,8–9 dorsal; iii,22–27 anal; i,5–6 pelvic and, i,4–13 pectoral (Tab. 1).

Juvenile period (Fig. 2G): In this period, the standard length ranges from 22.33 to 49.39 mm (mean ± SD = 29.56 mm ± 6.47). The body is compressed laterally, the eyes are large, the mouth is superior, the nostrils are double, and the anus is located posteriorly to the middle of the body. There is one large series of scales on the ventral keel and 32 to 35 scales arranged along the lateral line. The pectoral fins are long and only reach the origin of the pelvic fin. In preserved specimens, a dark dorsolateral band is observed extending from the snout to the caudal peduncle. In addition, dendritic and punctate chromatophores are present at the base of the inferior jaw, on the dentary, in the maxilla, around the eyes, and opercula. Pigmentation is distributed over the pectoral fin unbranched ray and between the dorsal and anal fin rays. The pelvic and adipose fins are hyaline, and the caudal fin color pattern is well defined, where the pigments are concentrated at the base and at the tip of the rays, however, the upper lobe is densely pigmented. Under of the body midline, pigmentation is scarce, when present, it is limited to the base of the anal fin and delineating the scales margin. The complete formation of the fins (branching and segmentation of the rays) occurs in this period, following the sequence: caudal, anal (iii, 26–28), dorsal (ii,8–9), pectoral (i,11–13), and pelvic (i,5–6).

In the preflexion stage, the body is long and low (14.34 to 19.41% of SL), becoming moderate in flexion (13.06 to 21.13% of SL), postflexion (19.64 to 27.30% of SL) and juvenile (28.20 to 30.86% of SL). The head is small in preflexion (18.36 to 24.12% of

SL) and flexion (19.24 to 26.59% of SL), becoming moderate in postflexion (25.14 to 31.59% of SL) and juvenile (24.61 to 30.25% of SL). Eyes range from moderate to large throughout early development (28.81 to 40.17% of HL). Snout length (SNL/HL), head depth (HD/HL), and distance of snout-dorsal (SND/SL), anal (SNA/SL), and pectoral (SNP/SL) fins, increased along the initial ontogeny, only the distance of snout-pelvic (SNV/SL) fins maintained its proportions (Tab. 1).

On growth patterns, the eye diameter exhibited continuous isometric development (linear regression) (Fig. 3B). The snout length had positive allometric growth (quadratic regression) (Fig. 3A). All other variables related to head length and standard length showed discontinuous isometric growth, therefore, they were better represented by the piecewise linear regression model. These variables showed an abrupt change in development after the breakpoint observed in the postflexion stage. For head length, the distance of snout-anal, dorsal, and pectoral fins the growth rate decreased after the breakpoint, while head deep, body deep, and distance of snout-pelvic fins increased growth velocity (Tab. 2; Fig. 3).

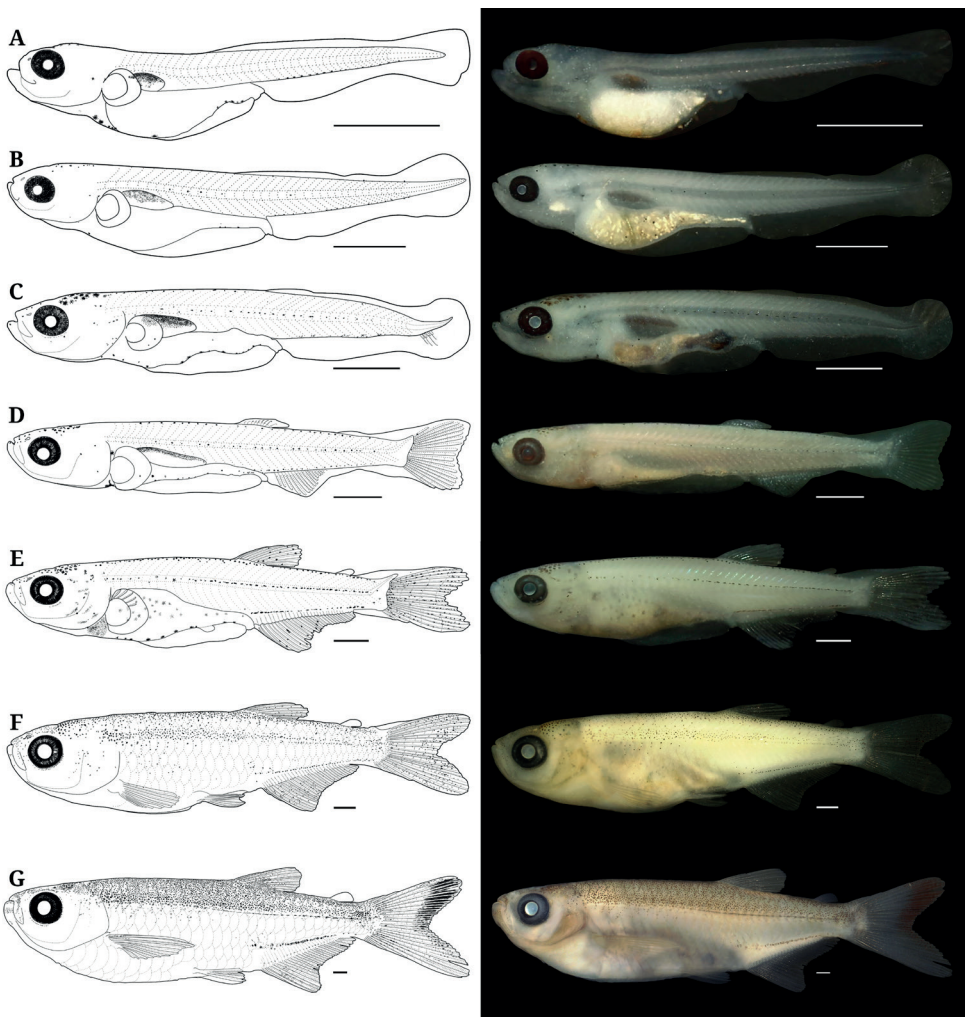

FIGURE 2 | Early development of *Triportheus albus*: (**A**) preflexion early (3.91 mm SL); (**B**) preflexion late (6.13 mm SL); (**C**) flexion early (7.01 mm SL), (**D**) flexion late (8.52 mm SL), (**E**) postflexion early (11.17 mm SL), (**F**) postlexion late (17.17 mm SL), and (**G**) juvenile (27.58 mm SL). Scale bar = 1 mm.

TABLE 1 | Variables analyzed (mm), minimum values (Min), maximum values (Max), mean (Mean), standard deviation (SD), and morphometric relationships (%) found for larvae and juveniles of *Triportheus albus*. Abbreviations: AF, absent fin; BD, body depth; BDA, depth body towards the anus; ED, eye diameter; HD, head depth; HL, head length; *N*, number of analyzed individuals; *n*, number of individuals with the mode of myomeres and rays; NV, not visible; SL, standard length; SNA, snout distance to the anal fin; SND, snout distance to the dorsal fin; SNL, snout length; SNP, snout distance to the pectoral fin; SNV, snout distance to the pelvic fin.

Variables (mm)	*Triportheus albus*							
	Larval period						Juvenile period (N = 16)	
	Preflexion (N = 25)		Flexion (N = 18)		Postflexion (N = 45)			
	Min-Max	Mean±SD	Min-Max	Mean±SD	Min-Max	Mean±SD	Min-Max	Mean±SD
SL	3.29-6.13	4.74±0.77	6.15-9.13	7.73±0.95	10.22-18.91	13.82±2.63	22.33-49.39	29.56±6.47
SND	1.54-3.05	2.21±0.43	2.86-5.17	4.11±0.66	6.15-11.33	8.11±1.55	13.08-28.59	17.45±3.72
SNA	1.92-3.66	2.70±0.46	3.43-5.96	4.70±0.80	6.71-12.38	9.01±1.72	14.24-33.55	19.60±4.49
SNP	0.69-1.32	0.95±0.16	1.10-2.11	1.65±0.32	2.35-5.03	3.49±0.75	5.38-13.64	7.57±1.85
SNV	NA	NA	NA	NA	5.07-9.56	6.73±1.24	10.49-22.21	14.23±2.85
HL	0.75-1.28	1.02±0.15	1.22-2.38	1.71±0.33	2.65-5.67	3.85±0.89	5.61-13.24	7.93±1.69
SNL	0.10-0.26	0.17±0.04	0.13-0.41	0.27±0.08	0.38-0.99	0.65±0.16	0.85-2.42	1.46±0.35
ED	0.25-0.43	0.36±0.04	0.41-0.82	0.61±0.12	0.97-1.88	1.29±0.25	2.01-4.48	2.76±0.56
HD	0.52-0.90	0.73±0.09	0.77-1.76	1.13±0.24	1.89-4.02	2.70±0.63	4.95-10.88	6.68±1.41
BD	0.60-1.09	0.73±0.12	0.94-1.89	1.21±0.25	2.20-5.15	3.27±0.89	6.62-14.51	8.80±1.99
BDA	0.27-0.60	0.44±0.10	0.46-1.22	0.84±0.19	1.74-3.95	2.55±0.71	5.19-11.06	6.92±1.41
Relations (%)								
BD/SL	14.34-19.41	17.42±1.34	13.06-21.13	15.65±2.04	19.64-27.30	23.35±2.15	28.20-30.86	29.71±0.79
BDA/SL	7.72-11.31	9.04±0.90	7.40-13.60	10.71±1.31	15.43-21.12	18.19±1.73	22.15-25.13	23.45±0.78
HD/BD	72.79-99.26	89.11±6.70	70.94-100	93.02±7.07	76.66-92.83	83.46±3.98	72.35-84.09	76.24±2.80
HD/BDA	129.10-211.63	172.74±20.95	123.09-169.01	135.94±11.21	96.20-119.26	107.17±5.83	90.86-101.67	96.59±2.79
HL/SL	18.36-24.12	21.63±1.30	19.24-26.59	22.03±2.04	25.14-31.59	27.73±1.64	24.61-30.25	26.91±1.50
ED/HL	31.07-40.13	35.79±2.56	32.67-40.05	35.39±1.69	28.81-37.30	33.87±2.10	30.53-40.17	34.93±2.20
HD/HL	61.37-76.14	71.55±3.57	59.24-75.82	65.86±5.42	64.44-76.79	70.08±2.96	73.19-94.70	84.39±4.97
SNL/HL	12.22-20.54	16.27±2.38	10.34-23.96	15.60±3.25	12.50-20.58	16.49±1.98	15.17-21.91	18.32±1.94
SND/SL	41.43-51.37	46.72±2.52	43.88-57.77	52.99±3.49	57.07-62.36	58.73±1.10	56.74-60.39	59.07±0.85
SNA/SL	54.59-59.72	56.98±1.54	55.49-67.10	60.53±3.49	63.33-68.29	65.19±1.19	63.77-67.93	66.21±1.01
SNP/SL	17.64-22.25	20.09±1.22	16.89-24.88	21.15±2.06	22.39-29.32	25.18±1.62	23.40-27.67	25.52±1.18
SNV/SL	NV	NV	NV	NV	44.38-53.97	48.81±1.82	44.97-50.29	48.28±1.50
Myomeres		**Mode**		**Mode**		**Mode**		
Preanal	18-19	18 (n = 16)	18-22	21 (n = 11)	21-22	21 (n = 23)	NV	NV
Postanal	19-21	20 (n = 14)	17-20	18 (n = 10)	17-18	17 (n = 17)	NV	NV
Total	38-39	38 (n = 13)	38-39	39 (n = 12)	38-39	39 (n = 17)	NV	NV
Number of rays								
Dorsal	AF	AF	9-10	10 (n = 3)	ii, 8-9	ii, 9 (n = 35)	ii, 8 - 9	ii, 9 (n = 13)
Anal	AF	AF	19-26	24 (n = 1)	iii, 22-28	iii, 27 (n = 23)	iii, 26- 28	iii, 27 (n = 8)
Pelvic	AF	AF	AF	AF	i, 5-6	i, 6 (n = 15)	i, 5 - 6	i, 6 (n = 8)
Pectoral	AF	AF	AF	AF	i, 4-13	i,13 (n = 16)	i, 11-13	i, 12 (n = 7)

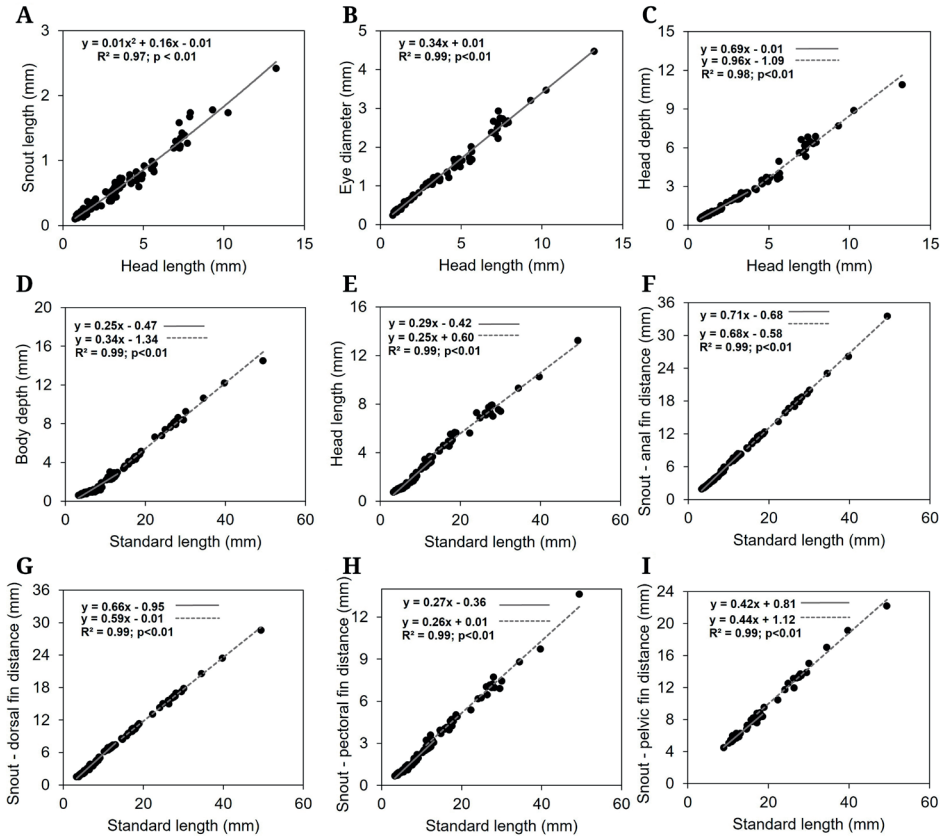

FIGURE 3 | Body ratios (mm) between head length and snout length (**A**), eye diameter (**B**), and head depth (**C**), and standard length and body depth (**D**), head length (**E**), distance from snout to anal fin (**F**), distance from snout to dorsal fin (**G**), distance from snout to pectoral fin (**H**) and distance from snout to pelvic fin (**I**) during the early development of *Triportheus albus*.

TABLE 2 | Values of Linear (L), quadratic (Q) and piecewise (S) regression analyzes of morphometric variables in relation to head length (HL) and standard length (SL) of *Triportheus albus* larvae and juveniles. R^2 = coefficient of determination. BM = best model, BP = breaking point (mm), a and b = regression parameters and N = number of individuals analyzed. Values in bold represent a significant difference ($p < 0.05$).

Triportheus albus												
Measured	R^2			Test F			BM	BP	a1	b1	a2	b2	N
	L	Q	S	Q/L	S/Q	S/L							
SNL/HL	0.97	0.97	0.97	**4.60**	3.44	**4.08**	Q	-	-0.01	0.16	-	-	104
ED/HL	0.99	0.99	0.99	0.83	**4.36**	2.61	L	-	0.01	0.34	-	-	104
HD/HL	0.98	0.98	0.99	**22.64**	**31.22**	**30.35**	S	2.57	0.69	-0.01	0.96	-1.09	104
BD/SL	0.99	0.99	0.99	**9.01**	**57.53**	**35.82**	S	3.18	0.25	-0.47	0.34	-1.34	104
HL/SL	0.99	0.99	0.99	**29.82**	**43.36**	**42.91**	S	3.43	0.29	-0.42	0.25	0.60	104
SNA/SL	1.00	1.00	1.00	0.00	**11.26**	**5.63**	S	8.38	0.71	-0.68	0.68	-0.58	104
SND/SL	1.00	1.00	1.00	**66.67**	**5.85**	**37.87**	S	7.44	0.66	-0.95	0.59	-0.01	104
SNP/SL	0.99	0.99	0.99	0.00	**13.91**	**6.95**	S	3.19	0.27	-0.36	0.26	0.01	104
SNV/SL	0.99	0.99	0.99	**8.41**	**10.63**	**10.22**	S	8.63	0.42	0.81	0.44	1.12	61

Triportheus angulatus

Larval period. Preflexion (Figs. 4A–B): The standard length ranges from 4.09 to 6.02 mm (mean ± SD = 4.69 mm ± 0.43). The rectilinear notochord is visible through transparency, and remnants of the yolk sac are still present. The body is elongated in a fusiform shape, convex and the head depth is generally greater than the body depth (HD/BD - 94.86 to 111.82%, mean ± SD = 102.98 ± 3.97%). The snout is rounded, and the mouth is terminal, but at the end of the stage (~5.00 mm SL) it becomes superior. The inferior jaw is short and barely visible in the dorsal view. The nostrils are simple, and the opercula are formed. The eyes are spherical and completely pigmented. The swim bladder is inflated and occupies a great space in the abdomen. The intestine is functional, straight and elongated, with the anus located in the body middle region. Individuals smaller than 4.60 mm SL have a few chromatophores in the occipital region (from one to three pigments); a horizontal line of pigments is noted to extend between the posterior region of the eye and the end of the operculum, analogous to a mask. Pigments are concentrated on the upper of the swim bladder and anteroventral portion of the digestive tract and spaced along the ventral region after the anus. In larger individuals (~5.00 mm SL) the coloration intensifies, and various dendritic pigments are distributed from the cephalic region to approximately the origin of the embryonic fin. Scarce dendritic pigments appear parallel to the notochord, and in the lower part of the intestine. The finfold is hyaline and can be seen enveloping the body dorsoventrally, from the first half of the intestine, posterior to digestive tract, to the origin of the pectoral fin button (SND/SL - 34.16 to 41.00%, mean ± SD = 37.07 ± 2.21). Only the pectoral fin button is evident. The total number of myomeres ranges from 37 to 39 (17–19 preanal and 19–22 postanal).

Flexion (Figs. 4C–D): The standard length ranges from 6.12 to 9.61 mm (mean ± SD = 7.41 mm ± 0.68). The notochord tip is flexed by the appearance of the hypural plate and there are no more remnants of the yolk. The form of the body is initially similar to the preflexion stage and, as it develops, it acquires an angular shape, with the anterior region clearly deeper than the posterior. The snout, mouth, maxilla, nostrils, eyes, swim bladder, and pectoral fin showed no changes with the preflexion stage. The anus is in the region posterior to the middle of the body. The color pattern is similar to the previous stage, however, there is the appearance of dendritic pigments throughout the dorsal region arranged in a series that intensifies with development. Along the intestine, the pigments are conspicuous and almost continuous. Midline body pigments become more visible, reaching the urostyle and sometimes around it. On flanks with approximately 9.00 mm SL, a row of internal melanophores parallel to the notochord emerges over the epidermis as continuous filiform chromatophores, extending from the caudal peduncle to the beginning of the operculum. Dendritic chromatophores are distributed between the caudal fin rays, but in greater concentrations at the median rays base. A continuous filiform band traced the base of the anal fin. Pigments can be observed on the snout, surrounding the premaxillary, under the dentary, base of the mandible, maxilla, nostrils, around the eyes, inner part of the operculum, arches, and gill filaments, on the lateral surface of the digestive tract and intestine. Also, internal chromatophores appear along the cleithrum, which, in larger individuals (9.00 mm SL), surround the pectoral fin base, connect to the swim bladder melanophores. Still, in flexion, there is the delineation of

the odd fins and the formation of their rays, which at the end of the stage are mostly developed. Likewise, the embryonic membrane is observed only in the region of origin of the pelvic fin. The adipose fin is in development. The caudal rays begin to segment, and the shape of the caudal fin is modified, initiating the division into two lobes. The myomeres total number ranges from 37 to 39 (18–22 preanal and 17–20 postanal).

Postflexion (Figs. 4E–F): The standard length ranges from 9.83 to 15.40 (mean ± SD = 11.94 mm ± 1.43). The notochord and swim bladder are no longer visible through transparency due to dense muscle tissue. The body profile remained the same. At the end of the phase, the nostrils are double. The pigmentation pattern is more intense in the previous stage. Numerous dark dendritic chromatophores appear on the flanks that outline and enhance the myomeres' pattern. Additionally, pigments are observed on the rays of the odd fins, including the adipose fin. The caudal fin stands out, where a dense pigmentation at the base of the rays is distributed along the median segments and is connected to a vertical strip arranged at the end of the caudal rays. The dorsal

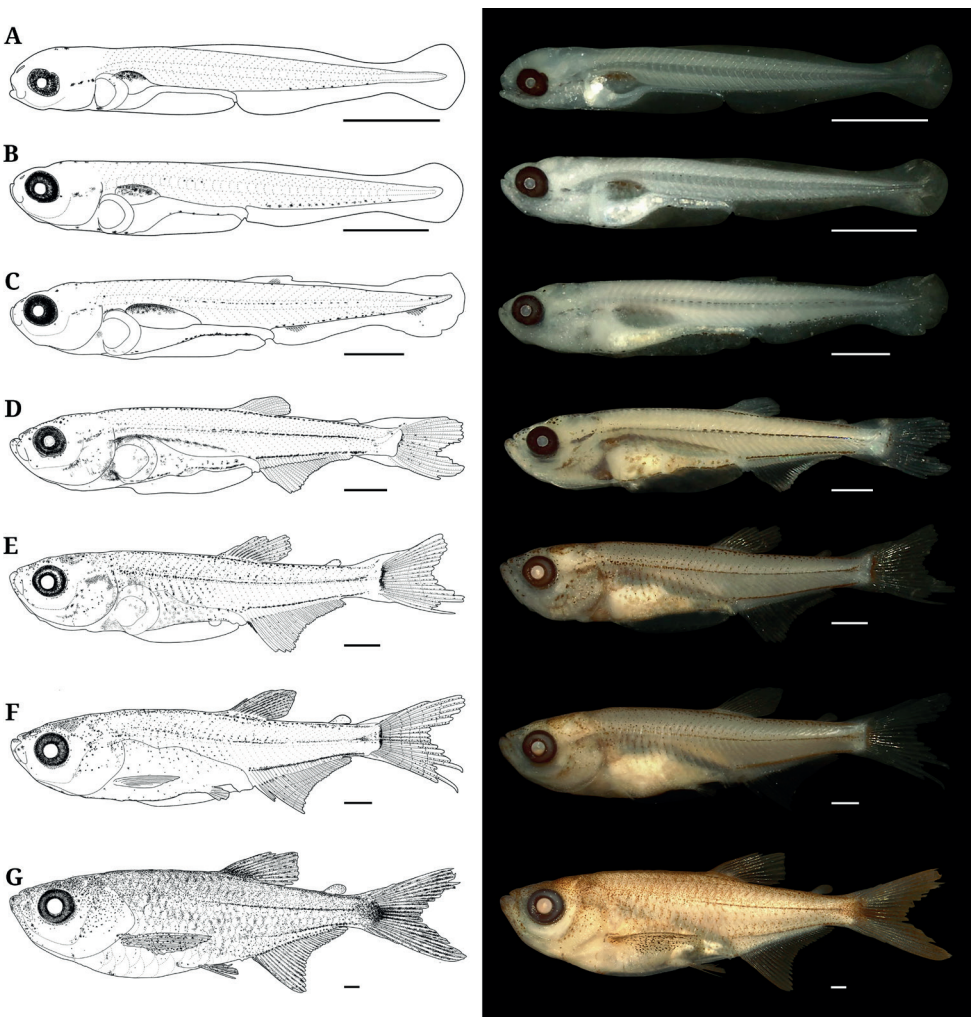

FIGURE 4 | Early development of *Triportheus angulatus*: (**A**) preflexion early (4.53 mm SL); (**B**) preflexion late (5.00 mm SL); (**C**) flexion early (7.50 mm SL), (**D**) flexion late (9.61 mm SL), (**E**) postflexion early (11.59 mm SL), (**F**) postflexion late (13.73 mm SL), and (**G**) juvenile (21.69 mm SL). Scale bar = 1 mm.

fin pigmentation is composed of filiform chromatophores in the basal part and circular dendritic in its distal portion. The dorsal, anal, and caudal fins are in the final stage of branching and segmentation of the flexible rays. The adipose fin is formed and embryonic membrane remains only in the ventral section, in contrast to the appearance of the pelvic fin that remains throughout the postflexion stage. At approximately 11.08 mm SL and 13.73 mm SL, the first pectoral fin rays and the pelvic fin rays appear, respectively, however, despite having developed rays, still do not have all the elements formed and segmented at the end of this stage. The myomeres total number varies from 38 to 39 (19–21 preanal and 17–19 postanal) and of unbranched and branched rays range from ii,9 dorsal, iii,27–30 anal, 5 pelvic, and i,6–8 pectoral (Tab. 3).

Juvenile period (Fig. 4G): Among the individuals, the standard length ranged from 18.08 to 53.71 mm (mean ± SD = 25.65 mm ± 6.70). The body is deep and compressed laterally, the eyes are large, the mouth is superior, the nostrils are double, and the anus is located posteriorly to the middle of the body. They have two series of large scales on the ventral keel and 34 to 37 scales along the lateral line. The pectoral fins are long, extending beyond the origin of the pelvic fin. Punctiform and dendritic pigmentation are distributed throughout the body. On the flanks, pigmentation outlines the edge of the scales. Chromatophores are distributed over the adipose fin and rays of all fins, including the pectoral and pelvic fins, which were previously hyaline. The color pattern of the caudal fin is notable, provides a band of chromatophores that are distributed from the base to the end of the median rays and is linked to a dark vertical stripe arranged in the distal region of the rays, acquiring the Y- shape. In this period of development, all fins are formed (branched and segmented) with the following formation sequence: caudal, anal (iii,27–31), dorsal (ii,9), pectoral (i,11–13), and pelvic (i,6).

The body is long and low in the preflexion stage (12.10 to 17.20% of SL) and varies for moderate in flexion (14.67 to 20.45% of SL), postflexion (18.46 to 25.04% of SL) and juvenile (28.02 to 35.16% of SL). The head length varies from small to moderate (17.58 to 32.78% of SL) and the eyes diameter varies from moderate to large (32.54 to 43.13% of HL) along the ontogeny. Head depth (HD/HL), snout length (SNL/HL), and distance of snout-fin pelvic (SNV/SL) maintained their proportions. The distance snout-fin dorsal (SND/SL), anal (SNA/SL), and pectoral (SNP/SL) distances increased during the ontogeny (Tab. 3).

Regarding growth pattern, the snout length, and the distance of snout-anal and ventral fins exhibited continuous isometric development (linear regression) (Figs. 5A, F, I). All other variables related to head length and standard length showed discontinuous isometric growth, therefore, they were better represented by the piecewise linear regression model. These variables underwent an abrupt change in development after the breakpoint, observed in the postflexion stage. For eye diameter, head length, distance snout-dorsal, and pectoral fins the growth rate decreased after the breakpoint, whereas head depth and body depth increased in growth velocity (Tab. 4; Figs. 5B, E, G and H, C, D).

TABLE 3 | Variables analyzed (mm), minimum values (Min), maximum values (Max), mean (Mean), standard deviation (SD), and morphometric relationships (%) found for larvae and juveniles of *Triportheus angulatus*. Abbreviations: AF, absent fin; BD, body depth; BDA, depth body towards the anus; ED, eye diameter; HD, head depth; HL, head length; *N*, number of analyzed individuals; *n*, number of individuals with the mode of myomeres and rays; NV, not visible; SL, standard length; SNA, snout distance to the anal fin; SND, snout distance to the dorsal fin; SNLs, snout length; SNP, snout distance to the pectoral fin; SNV, snout distance to the pelvic fin.

Variables (mm)	*Triportheus angulatus*							
	Larval period						Juvenile period (N = 30)	
	Preflexion (N = 46)		Flexion (N = 54)		Postflexion (N = 13)			
	Min-Max	Mean±SD	Min-Max	Mean±SD	Min-Max	Mean±SD	Min-Max	Mean±SD
SL	4.09-6.02	4.69±0.43	6.12-9.61	7.41±0.68	9.83-15. 40	11.94±1.43	18.08-53.71	25.65±6.70
SND	1.40-2.48	1.74±0.23	2.42-5.30	3.77±0.60	5.49-8.88	6.62±0.87	10.46-30.87	14.83±4.01
SNA	2.12-3.36	2.51±0.26	3.51-5.91	4.42±0.54	6.15-9.92	7.43±0.95	11.72-35.63	16.91±4.56
SNP	0.66-1.38	0.89±0.14	1.15-2.20	1.59±0.23	2.24-4. 01	2. 90±0.47	5.01-13.12	6.90±1.60
SNV	NA	NA	NA	NA	4.55-772	5.82±0.81	8.59-25.19	11.95±3.30
HL	0.75-1.23	0.92±0.12	1.12-2.37	1.65±0.26	2.25-4.12	3.07±0.47	5.22-13.51	7.50±1.58
SNL	0.10-0.20	0.14±0.03	0.13-0.36	0.23±0.05	0.33-0.66	0.49±0.10	0.82-2.27	1.31±0.36
ED	0.25-0.49	0.34±0.06	0.42-0.86	0.61±0.10	0.88-1.54	1.13±0.16	1.84-4.50	2.54±0.50
HD	0.55-0.97	0.69±0.11	0.95-1.87	1.25±0.17	1.85-3.54	2.50±0.45	4.25-12.92	6.27±1.75
BD	0.53-0.96	0.67±0.12	0.97-1.89	1.27±0.20	1.84-4.69	2.58±0.49	5.38-18.86	8.15±2.60
BDA	0.31-0.60	0.41±0.07	0.54-1.21	0.85±0.15	1.26-2.35	1.69±0.29	4.09-13.97	6.21±1.91
Relations (%)								
BD/SL	12.10-17.20	14.15±1.33	14.67-20.45	17.05±1.41	18.46-24.42	21.46±1.72	27.98-35.16	31.47±1.61
BDA/SL	7.46-10.96	8.62±0.79	8.26-14.36	11.19±1.22	12.50-15.24	14. 05±0.93	21.31-26.50	24.02±1.17
HD/BD	94.86-111.82	102.98±3.97	89.94-111.64	98.84±5.14	93.00-100.33	97.09±1.55	68.51-85.90	77.57±3.90
HD/BDA	146.73-189.17	168.89±9.96	122.47-192.27	151.34±13.99	139.25-165.12	148.27±6.65	92.52-115.97	101.65±5.19
HL/SL	17.58-21.94	19.52±1.15	17.69-25.99	22.15±1.77	22.49-27.04	25.62±1.40	25.15-32.78	29.47±1.80
ED/HL	32.54-41.88	36.39±2.35	33.12-43.13	37.01±2.05	34.50-39.23	36.75±1.44	30.69-40.12	34.08±2.24
HD/HL	66.25-84.50	74.41±4.03	66.50-98.30	76.20±5.87	77.58-87.53	81.26±3.07	71.50-102.06	83.04±6.50
SNL/HL	10.70-20.48	15.70±2.39	10.26-23.64	14.29±2.64	12.72-19.37	16.06±1.92	12.31-24.64	17.43±2.94
SND/SL	34.16-41.00	37.07±2.21	38.89-58.13	50.56±4.28	53.45-57.64	55.37±1.29	55.11-60.55	57.70±1.32
SNA/SL	51.04-57.43	53.42±1.54	55.19-63.75	59.51±2.25	60.56-64.43	61. 19±1.00	61.79-68.22	65.84±1.35
SNP/SL	16.14-22.93	18.83±1.42	18.19-24.23	21.36±1.35	20.60-26.17	24.17±1.81	23.46-30.80	27.05±1.68
SNV/SL	NV	NV	NV	NV	45.59-50.30	48.62±1.39	42.91-53.04	46.55±2.31
Myomeres		**Mode**		**Mode**		**Mode**		
Preanal	17-19	18 (n = 28)	18-22	20 (n = 17)	19-21	20 (n = 6)	NV	NV
Postanal	19-22	20 (n = 26)	17-20	18 (n = 17)	17-19	18 (n = 7)	NV	NV
Total	37-39	38 (n = 33)	37-39	38 (n = 29)	38-39	39 (n = 7)	NV	NV
Number of rays								
Dorsal	AF	AF	6 -11	10 (n = 7)	ii, 9	ii, 9 (n = 12)	ii, 9	ii, 9 (n = 30)
Anal	AF	AF	10 -29	10 (n = 3)	iii, 27 - 30	iii, 29 (n = 7)	iii, 27 - 31	iii, 30 (n = 9)
Pelvic	AF	AF	AF	AF	5	5 (n = 2)	i, 6	i, 6 (n = 30)
Pectoral	AF	AF	AF	AF	i, 6 - 8	7 (n = 1)	i, 11 - 13	i, 11 (n = 21)

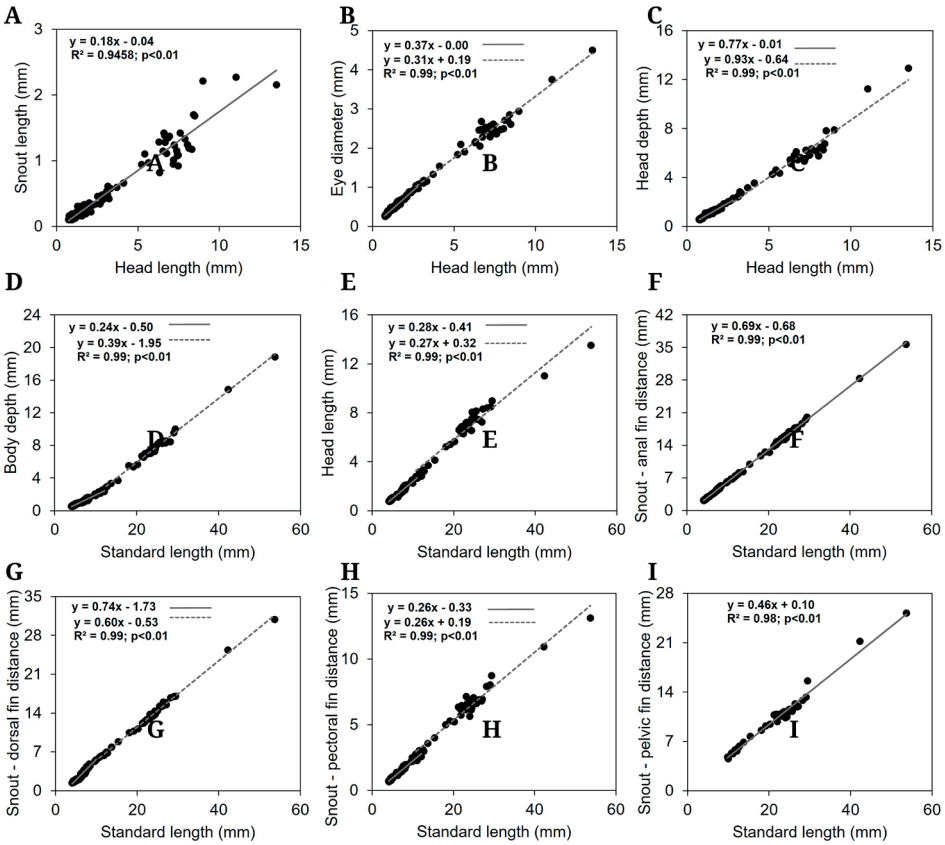

FIGURE 5 | Body ratios (mm) between snout length (**A**), head length and eye diameter (**B**), head depth (**C**), and standard length ratio (mm) between body depth (**D**), head length (**E**), distance from snout to anal fin (**F**), distance from snout to dorsal fin (**G**), distance from snout to pectoral fin (**H**) and distance from snout to pelvic fin (**I**) during the early development of *Triportheus angulatus*.

TABLE 4 | Values of Linear (L), quadratic (Q) and piecewise (S) regression analyzes of morphometric variables in relation to head length (HL) and standard length (SL) of *Triportheus angulatus* larvae and juveniles. R^2 = coefficient of determination. BM = best model, BP = breaking point (mm), a and b = regression parameters and N = number of individuals analyzed. Values in bold represent a significant difference ($p < 0.05$).

Triportheus angulatus												
Measured	R^2			Test F			BM	BP	a1	b1	a2	b2	N
	L	Q	S	Q/L	S/Q	S/L							
SNL/HL	0.95	0.95	0.95	0.26	**6.64**	3.45	L	-	-0.04	0.18	-	-	143
ED/HL	0.99	0.99	0.99	**11.42**	**9.29**	**10.70**	S	0.97	0.37	0.00	0.31	0.19	143
HD/HL	0.99	0.98	0.99	**73.01**	**-36.46**	**8.43**	S	2.24	0.77	-0.01	0.93	-0.64	143
BD/SL	0.99	0.99	1.00	**42.41**	**240.63**	**178.07**	S	2.64	0.24	-0.50	0.39	-1.95	143
HL/SL	0.99	0.98	0.99	**151.64**	**-51.16**	**21.79**	S	2.77	0.28	-0.41	0.27	0.32	143
SNA/SL	1.00	1.00	1.00	0.00	**-2.16**	-1.08	L	-	-0.68	0.69	-	-	143
SND/SL	1.00	1.00	1.00	**34.75**	**41.36**	**43.10**	S	5.70	0.74	-1.73	0.60	-0.53	143
SNP/SL	0.99	0.99	0.99	**65.94**	**-18.28**	**19.26**	S	2.60	0.26	-0.33	0.26	0.19	143
SNV/SL	0.98	0.98	0.98	3.12	0.45	1.76	L	-	0.10	0.46	-	-	43

Identification key for some *Triportheus* species from the Amazon basin during early ontogeny (Fig. 6)

1a. Less than 40 myomeres total number.....2

1b. More than 40 myomeres total number (Fig. 6D).....*Triportheus auritus* (see Cajado *et al*., 2021)

2a. Convex dorsal profile in early stage larvae (Fig. 6A); inner mediolateral band emerging in the epidermis in mostly dashed and continuous pigments (Fig. 6B); presence of evident angle between the anterior and posterior regions of the body in more developed larvae; conspicuous pigmentation on the median rays connecting to a vertical band at the tip of the caudal-fin rays (Fig. 6C).....*Triportheus angulatus*

2b. Concave dorsal profile in early stage larvae (Fig. 6A'); mediolateral band only in the epidermis, mostly in dotted pigments (Fig. 6B'); fusiform body without evident angle in more developed larvae; conspicuous pigmentation at the tip of the upper lobe of the caudal fin (Fig. 6C') ..... *Triportheus albus*

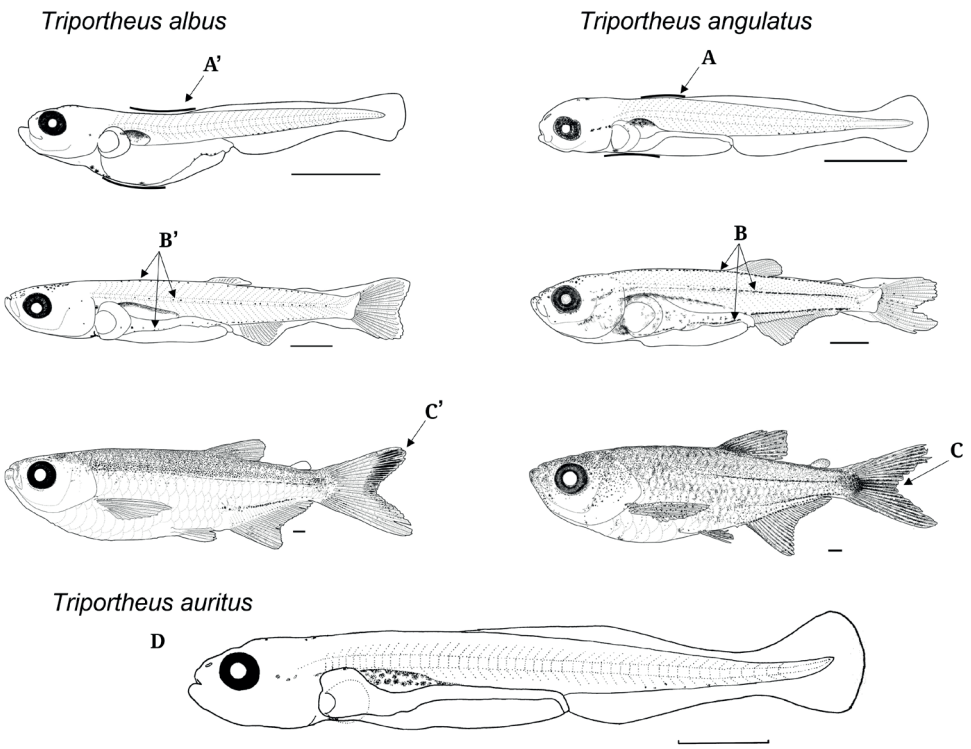

FIGURE 6 | Illustrated summary of the identification key for Amazonian *Triportheus* larvae. Letters explain characters mentioned in the identification key. Scale bars = 1 mm.

Morphometric comparisons. All variables related to head length, except for snout length, were significantly different between the two species (ANCOVA, $p < 0.05$), with eye diameter and head depth being higher in *T. angulatus* (Tab. 5). The variables head length and distance of snout-dorsal, anal, and pelvic fins differ among species. The distances of snout-anal and pelvic fins were greater in *T. albus* throughout the early ontogeny. The distance of snout-dorsal fin and head length is initially longer in *T. albus*, but these changes in the juvenile period, becoming longer in *T. angulatus* (Tabs. 1, 3).

Diagnosis between *Triportheus albus* and *T. angulatus*. In preflexion, *Triportheus albus* is distinguished from *T. angulatus* by the combination of a concave dorsal profile, superior mouth, exposed dentary in dorsal view, the head always shallower than the body, and SND/SL > 41.00% *vs*. convex dorsal profile, terminal mouth becoming superior at the end of preflexion, mandible barely visible in dorsal view, the head generally deeper than the body and SND/SL ≤ 41.00%. In the flexion stage *T. albus* is distinguished from *T. angulatus* by the absence of pigments in the urostyle, presence of a dotted band along the medial-lateral line of the body only in the epidermis, fusiform body, without a sharp angle between the anterior and posterior region of the body, and low and elongated head *vs*. presence of pigments in the urostyle, as well as a band of internal pigments parallel to the notochord emerging over the epidermis as dashed chromatophores, angular body, with the anterior region of the body clearly more robust than the posterior, high and short head. In postflexion and juvenile *T. albus* is distinguished from *T. angulatus* by the presence of chromatophores at the base of the caudal fin rays and at the tip of its lobes, the upper being generally more pigmented *vs*. existence of pigments on the median rays and in the distal region of the caudal fin and by the absence of overlap in the morphometric proportions during postflexion, such as BDA/SL, HD/BD, HD/BDA, HD/HL, and SND/SL (Tabs. 1–2).

TABLE 5 | Results of the analysis of covariance (ANCOVA) for the variables obtained in the individuals *Triportheus albus* and *Triportheus angulatus* in relation to standard and head length.

Measured	Intercept		Covariable categorical (species)		Covariable continuos (HL and SL)	
	F	P	F	P	F	P
SNL/HL	1985.51	<**.001**	0.201	0.655	3848.91	<**.001**
ED/HL	11888.3	<**.001**	22.3	<**.001**	23226.5	<**.001**
HD/HL	11740.2	<**.001**	78.7	<**.001**	23112.9	<**.001**
BD/SL	5538.939	<**.001**	0.472	0.493	10786.3	<**.001**
HL/SL	11195.87	<**.001**	4.97	**0.027**	21639.08	<**.001**
SNA/SL	69629.7	<**.000**	62.8	<**.000**	134254.7	<**.000**
SND/SL	13582.2	<**.001**	78.5	<**.001**	25832.7	<**.001**
SNP/SL	13464.64	<**.002**	0.275	0.601	26134.24	<**.001**
SNV/SL	787.2	<**.001**	21.2	<**.001**	1449.1	<**.001**

DISCUSSION

During the initial ontogeny *Triportheus albus* and *T. angulatus* presented common characteristics to the species of *Triportheus*, such as a pigmentation pattern composed of three longitudinal bands along the body (dorsal, mid-lateral, and ventral regions), eyes large to moderate, superior mouth, elongated intestine, and presence of ventral keel in more developed individuals (Nakatani *et al*., 2001; Garcia *et al*., 2016; Cajado *et al*., 2021). The larvae and juveniles of *T. albus* and *T. angulatus* can be diagnosed and differentiated from each other and from other congener species through the combination of color pattern, body shape, myomeres number, and morphometric relationships at each stage.

Triportheus albus larvae do not show any yolk remains in the preflexion stage. Alternatively, *T. angulatus* larvae still have traces of endogenous feeding (yolk sac). The presence of enduring endogenous reserves in *T. angulatus* can indicate greater chances of survival of this species in relation to *T. albus*. This would be an advantage in conditions of irregular and variable food supply, as occurs during the drift of the larvae of these species, before reaching the nursery sites in the floodplain (Ponte *et al*., 2016; Oliveira *et al*., 2020b; Mariac *et al*., 2022). Precisely because this condition allows a mixed feeding, that is, the larvae start to consume the food before the complete absorption of the endogenous reserve. This type of food acquisition and the time of its duration positively reflect on the development, growth, and survival of larvae (Bialetzki *et al*., 2001). However, the period of yolk sac absorption is highly variable among Neotropical fish species, such as Characiformes, and can be influenced by environmental conditions, availability of ideal food, and mainly by the evolutionary history of each species (Godinho *et al*., 2003; Marinho, 2017; Rocha *et al*., 2019).

Features such as eye pigmentation, digestive tract functionality, pectoral fin bud and swim bladder development occur concurrently in the preflexion larval stage for both species. These findings are consistent with other Neotropical Characiformes species (Lima *et al*., 2021; Oliveira *et al*., 2022; Ticiani *et al*., 2022), and are linked to the onset and efficiency of exogenous feeding. For example, pigmented eyes, an open mouth, and a functional gut are essential for locating, capturing, and absorption of food (Makrakis *et al*., 2005; Stevanato, Ostrensky, 2018), while the pectoral fin bud and swim bladder promote position control in the water column (Cajado *et al*., 2021; He *et al*., 2022). The superior positioning of the mouth (except during the beginning of preflexion for *T. angulatus*), reflects the trophic guild of adult individuals, which are omnivorous (Almeida, 1984; Ferreira *et al*., 1998; Yamamoto *et al*., 2004), indicating that these species consume a wide spectrum of trophic resources associated with the subsurface of the water column since its early development.

The intensification of pigmentation throughout the early ontogeny of *Triportheus* suggests camouflage adaptations in the environment (Cajado *et al*., 2021; Silva *et al*., 2021; Oliveira *et al*., 2022). This is supported because *Triportheus* larvae in early stages are essentially pelagic and poorly pigmented, but in more advanced stages, they are highly pigmented and occupy structured environments, such as aquatic vegetation and marginal regions (Zacardi *et al*., 2020a; Oliveira *et al*., 2020b; Cajado *et al*., 2020).

The pigmentation pattern stands out as a fundamental characteristic for the identification of Amazonian Characiformes, even for congener species (Araújo-Lima *et al*., 1993; Oliveira *et al*., 2022). However, the diagnosis of a species based on color

must be carried out in parsimony and associated with other factors, in view of the high interspecific similarity, species richness and limited knowledge about the initial stages of fish in the Amazon region (Zacardi *et al*., 2020b).

For *Triportheus*, the coloration associated with morphometric and meristic data can be a useful character in species identification during early ontogeny (Cajado *et al*., 2021). *Triportheus albus* larvae have few body pigments, most of which are speckled and non-continuous in the three body strips and absent in the urostyle. In contrast, *T. angulatus* larvae are highly pigmented in the final stages of development and have a pattern with internal pigments parallel to the midline of the body that emerges in the epidermis as dashed and continuous chromatophores, and on the urostyle. Demonstrating, therefore, that pigmentation is a fundamental element in distinguishing these species.

The sequence of complete development of the fins (caudal, anal, dorsal, pectoral, and pelvic) of *T. albus* and *T. angulatus* contrasts with other described Characiformes (Nakatani *et al*., 2001; Ponton, Mérigoux, 2001; Oliveira *et al*., 2022; Silva *et al*., 2022) in which the basic series of fin formation is primarily caudal, anal, dorsal, pelvic, and pectoral. However, it corroborates what was observed by Cajado *et al*. (2021) for another congener, *T. auritus*, reinforcing that the sequence of fin formation is an important character to diagnose the genus *Triportheus* during early development. Both species described here show overlap in count of myomeres total number (37–39 in *T. angulatus vs.* 38–39 in *T. albus*) therefore, this character cannot be used efficiently to diagnose the two species. Moreover, it can be useful for differentiating from another congener sympatric species of the Amazon basin, *T. auritus*, which has 45 to 48 myomeres total number (Cajado *et al*., 2021).

The different growth models observed for the SNL/HL, ED/HL, SNV/SL, and SNA/SL relationships between the two *Triportheus* reflect the adaptive ontogenetic development in response to ecological requirements and indicate that these individuals exploit environmental and trophic resources distinct during the early stages of life. This is because they mainly related the development of these parameters to vision, feeding, and active swimming (Santos *et al*., 2020; Oliveira *et al*., 2022; Silva *et al*., 2022).

The discontinuous isometric growth for the variables HD, BD, HL, SND, and SNP with the breakpoint in the postflexion stage was similar for both species. This indicates that the greatest changes in ecomorphological aspects occur during this phase. The increase in the growth rate of head depth in more developed individuals suggests changes in exogenous eating habits (Silva *et al*., 2022). The increase in body height and decrease in the rate of growth of head length demonstrate greater development of musculature and remodeling of body morphology (*e.g*., emergence of the ventral keel and bone elements) (Oldani, 1979; Santos *et al*., 2020). These changes, associated with the formation of fins, contribute to swimming efficiency, and prey capture and consequently cause changes in the functional characteristics of the species, such as position in the water column and trophic level (Oliveira, Suzuki *et al*., 2020; Silva *et al*., 2021; Cajado *et al*., 2021).

The reduction in the growth rate of the SND and SNP demonstrates the little development of these parameters after the transition to the juvenile period, as observed by Cajado *et al*. (2021) for *T. auritus*, due to ossification of the ribs, coracoid, and cleithrum, the emergence of pterygiophores, and the intensification of the body musculature. Some authors suggest that these morphological changes strongly influence

on the locomotion and position of the fins throughout the ontogenetic phases (Santos *et al*., 2020; Jin *et al*., 2021).

In conclusion, the integrative regressive sequence approach made it possible, through meristic, morphological, and morphometric characters, to accurately identify the larvae and juveniles of the two species of *Triportheus* at each stage. The greatest body metamorphoses occur at the threshold between the larval and juvenile period (postflexion) linked to ecomorphological and functional changes, such as eating habits, efficiency in swimming activity, and position in the water column. Despite the complexity of the identification, the information presented in this study is consistent with the recognition of these two species, contributing to taxonomy, systematics, and ecological, studies, for the management and conservation of these fish with the potential for fishing exploitation.

ACKNOWLEDGMENTS

The authors would like to thank colleagues at the Universidade Federal do Oeste do Pará, represented by the Laboratório de Ecologia do Ictioplâncton e Pesca em Águas Interiores (https://leipaiufopa.com), for their assistance in collecting, sorting, and identifying the larvae and juveniles used in this study, and to the The Nature Conservancy of Brazil for financial and logistical support through the "Águas do Tapajós" Project which enabled us to collect larvae and juveniles in the Tapajós River. DMZ thanks the Ministério da Ciência e Tecnologia (MCT) and the Instituto Mamirauá de Desenvolvimento Sustentável (ISDM).

REFERENCES

- **Ahlstrom EH, Butler JL, Sumida BY.** Pelagic stromateoid fishes (Pisces, Perciformes) of the eastern Pacific: kinds, distributions, and early life histories and observations on five of these from the northwest Atlantic. Bull Mar Sci. 1976; 26(3):285–402.
- **Almeida RG.** Biologia alimentar de três espécies de *Triportheus* (Pisces: Characoideil, Characidae) do Lago do Castanho, Amazonas. Acta Amaz. 1984; 14(1–2):48–76. https://doi.org/10.1590/1809-43921984142076
- **Araújo JDA, Ghelfi A, Val AL.** *Triportheus albus* Cope, 1872 in the blackwater, clearwater, and whitewater of the Amazon: A case of phenotypic plasticity? Front Genet. 2017; 8(114):1–12. https://doi.org/10.3389/fgene.2017.00114
- **Araújo-Lima CARM, Kirovsky AL, Marca AG.** As larvas dos pacus, *Mylossoma* spp. (Teleostei; Characidae), da Amazônia Central. Braz J Biol. 1993; 53:591–600.
- **Batista VS, Isaac VJ, Fabré NN.** A produção desembarcada por espécie e sua variação por macrorregião Amazônica. In: Batista VS, Isaac VJ, editors. Peixes e pesca no Solimões-Amazonas: uma avaliação integrada. 2012. Brasília: ProVárzea/ IBAMA.
- **Bialetzki A, Baumgartner G, Sanches PV, Galuch AV, Luvisuto MA, Nakatani K *et al*.** Caracterização do desenvolvimento inicial de *Auchenipterus osteomystax* (Osteichthyes, Auchenipteridae) da bacia do rio Paraná, Brasil. Acta Sci Biol Sci. 2001; 23:377–82.
- **Cajado RA, Oliveira LS, Suzuki MPL, Zacardi DM.** Spatial diversity of ichthyoplankton in the lower stretch of the Amazon River, Pará, Brazil. Acta Ichthyol Piscat. 2020; 50(2):127–37. https://doi.org/10.3750/AIEP/02786

- **Cajado RA, Oliveira LS, Silva FKS, Zacardi DM.** Early development of the Neotropical fish known as long sardine *Triportheus auritus* (Valenciennes, 1850) (Characiformes, Triportheidae). J Appl Ichthyol. 2021; 37(5):759–69. https://doi.org/10.1111/jai.14228
- **Dagosta FCP, Pinna M.** The fishes of the Amazon: distribution and biogeographical patterns, with a comprehensive list of species. Bull Am Mus Nat Hist. 2019; 431:1–163. https://doi.org/10.1206/0003-0090.431.1.1
- **Doria CRC, Queiroz LJ.** A pesca comercial das sardinhas (*Triportheus* spp.) desembarcadas no mercado pesqueiro de Porto Velho, Rondônia (1990-2004): produção pesqueira e perfil geral. Biotemas. 2008; 21(3):99–106. https://doi.org/10.5007/2175-7925.2008v21n3p99
- **Ferraz PS, Barthem RB.** Estatística do monitoramento do desembarque pesqueiro na região de Tefé Médio Solimões: 2008–2010. 2nd ed. Tefé: Instituto de Desenvolvimento Sustentável Mamirauá; 2016; 68–70.
- **Ferreira EJG, Zuanon JA, Santos GM.** Peixes comerciais do médio Amazonas: região de Santarém, Pará. Brasília: IBAMA; 1998.
- **Fricke R, Eschmeyer WN, Van der Laan R.** Eschmeyer's catalog of fishes: genera, species, references [Internet]. San Francisco: California Academy of Science; 2022. Available from: https://researcharchive.calacademy.org/research/ichthyology/catalog/fishcatmain.asp
- **Garcia DAZ, Claro-García A, Costa ADA, Bialetzki A, Casimiro ACR, Swarça AC *et al*.** Composição ictiofaunística e ontogenia inicial das espécies. In: Orsi ML, Almeida FS, Swarça AC, Claro-García A, Vianna NC, Garcia DAZ *et al*., editors. Ovos, larvas e juvenis dos peixes da bacia do rio Paranapanema: uma avaliação para a conservação. 1st ed. Assis: Triunfal Gráfica e Editora; 2016.
- **García-Dávila CR, Riveiro H, Flores MA, Loayza JEM, Angulo CAC, Castro D *et al*.** Peces de consumo de la amazonía peruana. 2018. Available from: https://investigacion.minam.gob.pe/observatorio/sites/default/files/garcia_libro_2018.pdf
- **Godinho HP, Santos JE, Sato Y.** Ontogênese larval de cinco espécies de peixes do São Francisco. In: Godinho HP, Godinho AL, editors. Águas, peixes e pescadores do São Francisco das Minas Gerais. Belo Horizonte: PUC Minas; 2003. p.133–48.
- **He Y, Liang X-F, Guo W, Tian C, Sun L, Huang K *et al*.** Swimbladder non-inflation and its influence on larviculture of mandarin fish (*Siniperca chuatsi*). Aquac Rep. 2022; 23:101057. https://doi.org/10.1016/j.aqrep.2022.101057
- **Imbiriba LC, Coelho YKS, Serrão EM, Zacardi DM.** Ictiofauna acompanhante associada a pesca do camarão-da-amazônia *Macrobrachium amazonicum* (Heller, 1862) (Decapoda, Palaeomonidae): subsídios para gestão ambiental e ordenamento da pesca. G Sci. 2020; 14(4):52–73. https://doi.org/10.22478/ufpb.1981-1268.2020v14n4.52766
- **Isaac VJ, Castello L, Santos PRB, Ruffino ML.** Seasonal and interannual dynamics of river-floodplain multispecies fisheries in relation to flood pulses in the Lower Amazon. Fish Res. 2016; 183:352–59. https://doi.org/10.1016/j.fishres.2016.06.017
- **Jin D-S, Park J-M, Baek J-I, Han K-H.** Osteological development of the larvae and juvenile of *Favonigobius gymnauchen* (Pisces:Gobiidae). Dev Reprod. 2021; 25(1):33–41. https://doi.org/10.12717/DR.2021.25.1.33
- **Kováč V, Copp GH, Francis MP.** Morphometry of the stone loach, *Barbatula barbatula*: do mensural characters reflect the species' life history thresholds? Environ Biol Fish. 1999; 56:105–15. https://doi.org/10.1023/A:1007570716690
- **Leis JM, Trnski T.** The larvae of Indo-Pacific shorefishes. Honolulu: University of Hawaii Press; 1989.
- **Lima DLG, Cajado RA, Silva LVF, Maia JLS, Zacardi DM.** Descrição morfológica do desenvolvimento inicial de *Brycon amazonicus* (Characiformes, Bryconidae) do Baixo Amazonas, Pará. Biota Amaz. 2021; 11(1):60–67.
- **Lopes D.** Taxonomia de *Triportheus* Cope, 1872 (Ostariophysi, Triportheidae) da bacia Platina. [Master Dissertation]. Campo Grande: Universidade Federal de Mato Grosso do Sul; 2020.

- **Makrakis MC, Nakatani K, Bialetzki A, Sanches PV, Baumgartner G, Gomes LC.** Ontogenetic shifts in digestive tract morphology and diet of fish larvae of the Itaipu Reservoir, Brazil. Environ Biol Fish. 2005; 72:99–107. https://doi.org/10.1007/s10641-004-6596-9
- **Malabarba MCSL.** Revision of the Neotropical genus *Triportheus* Cope, 1872 (Characiformes: Characidae). Neotrop Ichthyol. 2004; 2(4):167–204. https://doi.org/10.1590/S1679-62252004000400001
- **Mariac C, Renno JF, Garcia-Davila C, Vigouroux Y, Mejia E, Angulo C *et al.*** Species-level ichthyoplankton dynamics for 97 fishes in two major river basins of the Amazon using quantitative metabarcoding. Mol Ecol. 2022; 31(6):1627–48. https://doi.org/10.1111/mec.15944
- **Marinho MMF.** Comparative development in *Moenkhausia pittieri* and *Paracheirodon innesi* (Ostariophysi: Characiformes) with comments on heterochrony and miniaturization in the Characidae. J Fish Biol. 2017; 91(3):851–65. https://doi.org/10.1111/jfb.13384
- **Nakatani K, Agostinho AA, Bialetzki A, Baumgartner G, Sanches PV, Makrakis M *et al***. Ovos e larvas de peixes de água doce: desenvolvimento manual de identificação. Maringá: EDUEM; 2001.
- **Oldani N.** Identificación y morfología de larvas y juveniles de *Triportheus paranensis* (Günther, 1874). (Pisces, Characidae). Nat Neotrop. 2005; 1:61–71.
- **Oliveira CC, Suzuki MAL, Oliveira LS, Zacardi DM.** Description of the initial development and temporal distribution of *Microphilypnus tapajosensis* larvae and juveniles in a reservoir in the Eastern Amazon. Ci Nat. 2020b; 42:e49. https://doi.org/10.5902/2179460X41542
- **Oliveira LS, Cajado RA, Santos LRB, Suzuki MAL, Zacardi DM.** Bancos de macrófitas aquáticas como locais de desenvolvimento das fases iniciais de peixes em várzea do Baixo Amazonas. Oecol Aust. 2020a; 24(3):644–60. https://doi.org/10.4257/oeco.2020.2403.09
- **Oliveira LS, Cajado RA, Silva FKS, Andrade MC, Zacardi DM.** Early development of two commercially valuable fish from the lower Amazon River, Brazil (Characiformes: Serrasalmidae). Neotrop Ichthyol. 2022; 20(1):e210024. https://doi.org/10.1590/1982-0224-2021-0024
- **Ponte SCS, Ferreira LC, Bittencourt SCS, Queiroz HL, Zacardi DM.** Variação espacial e temporal das larvas de *Triportheus* (Characiformes, Triportheidae), no médio Rio Solimões, Amazônia Central, Brasil. Acta Fish Aquat Res. 2016; 4(2):71–81. https://doi.org/10.2312/ActaFish.2016.4.2.71-81
- **Ponton D, Mérigoux S.** Description and ecology of some early life stages of fishes in the river Sinnamary (French Guiana, South America). Folia Zool. 2001; 50:1–116. Available from: https://horizon.documentation.ird.fr/exl-doc/pleins_textes/divers21-03/010027147.pdf
- **Reynalte-Tataje DA, Lopes CA, Massaro MV, Hartmann PB, Sulzbacher R, Santos JA *et al.*** State of the art of identification of eggs and larvae of freshwater fish in Brazil. Acta Limnol Bras. 2020; 32:e6. https://doi.org/10.1590/s2179-975x5319
- **Rocha MSA, Silva RC, Santos JCE, Schorer M, Nascimento MP, Pedreira MM.** Comparative larval ontogeny of two fish species (Characiformes and Siluriformes) endemic to the São Francisco River in Brazil. J Fish Biol. 2019; 96(1):49–58. https://doi.org/10.1111/jfb.14185
- **Santos JA, Soares CM, Bialetzki A.** Early ontogeny of yellowtail tetra fish *Astyanax lacustris* (Characiformes: Characidae). Aquac Res. 2020; 51(10):4030–42. https://doi.org/10.1111/are.14746
- **Silva FKS, Cajado RA, Oliveira LS, Ribeiro FRV, Zacardi DM.** Early ontogeny of *Pimelodus blochii* Valenciennes, 1840 (Siluriformes: Pimelodidae): Neotropical catfish. Zootaxa. 2021; 4948(1):83–98. https://doi.org/10.11646/zootaxa.4948.1.4
- **Silva FKS, Cajado RA, Oliveira LS, Santos Z, Santos JA, Silva LVF *et al.*** Early development of *Prochilodus nigricans* Spix & Agassiz, 1829 (Characiformes: Prochilodontidae) in captivity. Aquac Res. 2022; 53(12):4540–55. https://doi.org/10.1111/are.15951
- **Silvano RAM, Nitschke PP, Vieira KC, Nagl P, Martínez ATR, Chuctaya JA *et al.*** Atlas of fish of Tapajós and Negro rivers I: Characiformes. In: Silvano RAM, editor. Fish and fisheries in the Brazilian Amazon: people, ecology and conservation in black and clear water rivers. Springer Cham. 2020. p.41–196.
- **Stevanato DJ, Ostrensky A.** Ontogenetic development of tetra *Astyanax lacustris* (Characiformes: Characidae). Neotrop Ichthyol. 2018; 16(2):e170073. https://doi.org/10.1590/1982-0224-20170073

- **Ticiani D, Delariva RL, Iquematsu MS, Bialetzki A.** Larval development of *Characidium orientale* (Actinopterygii: Crenuchidae) a small Neotropical fish. Iheringia, Sér Zool. 2022; 112:e2022003. https://doi.org/10.1590/1678-4766e2022003
- **Van der Sleen P, Zanata A.** Family Triportheidae - elongate hatchetfishes and relatives. In: Albert JS, Van der Sleen P, editors. Field Guide Amazon Orinoco and Guianas. Princeton University Press; 2018. p.196–98.
- **Yamamoto KC, Soares MGM, Freitas CEC.** Alimentação de *Triportheus angulatus* (Spix & Agassiz, 1829) no lago Camaleão, Manaus, AM, Brasil. Acta Amaz. 2004; 34(4):653–59. https://doi.org/10.1590/S0044-59672004000400017
- **Zacardi DM.** A pesca artesanal em áreas de inundação no Baixo Amazonas, Pará: técnicas de captura e composição pesqueira. In: Oliveira AC, editor. Aquicultura e pesca: adversidades e resultados. 3rd ed. Ponta Grossa: Atena; 2020. p.1–16.
- **Zacardi DM, Bittencourt SCS, Queiroz HL.** Recruitment of migratory Characiforms in the different wetland habitats of Central Amazonia: subsidies for sustainable fisheries management. J Appl Ichthyol. 2020a; 36(4):431–38. https://doi.org/10.1111/jai.14040
- **Zacardi DM, Santos JA, Oliveira LS, Cajado RA, Pompeu PS.** Ichthyoplankton studies as referential for the management and monitoring of fishery resources in the Brazilian Amazon basin. Acta Limnol Bras. 2020b; 32:e203. https://doi.org/10.1590/s2179-975x6619

AUTHORS' CONTRIBUTION

Ruineris Almada Cajado: Conceptualization, Formal analysis, Investigation, Writing-original draft.

Fabíola Katrine Souza da Silva: Formal analysis, Investigation, Writing-review and editing.

Lucas Silva de Oliveira: Conceptualization, Formal analysis, Visualization, Writing-review and editing.

Zaqueu dos Santos: Investigation, Methodology.

Andréa Bialetzki: Validation, Writing-review and editing.

Diego Maia Zacardi: Data curation, Methodology, Resources, Supervision, Validation, Writing-review and editing.

ETHICAL STATEMENT

The license for the collection of biological material was granted by the Sistema de Autorização e Informação em Biodiversidade (SISBIO) of the Instituto Chico Mendes de Conservação da Biodiversidade and Ministério do Meio Ambiente of Brazil, authorizations numbers 75271-1/2020, 72330 and 23741-1, issued based on the Normative Instruction no. 154/2007.

COMPETING INTERESTS

The author declares no competing interests.

HOW TO CITE THIS ARTICLE

- **Cajado RA, Silva FKS, Oliveira LS, Santos Z, Bialetzki A, Zacardi DM.** Early life history of two Neotropical Triportheidae fish (Characiformes). Neotrop Ichthyol. 2023; 21(1):e220102. https://doi.org/10.1590/1982-0224-2022-0102

Neotropical Ichthyology

OPEN ACCESS

This is an open access article under the terms of the Creative Commons Attribution License, which permits use, distribution and reproduction in any medium, provided the original work is properly cited.

Distributed under
Creative Commons CC-BY 4.0

© 2023 The Authors.
Diversity and Distributions Published by SBI

Official Journal of the
Sociedade Brasileira de Ictiologia
SBI